https://doi.org/10.5194/angeo-2024-19
Preprint. Discussion started: 2 December 2024

Annales Geophysicae Discussions
Open Access
EGU

The Magnetic Vortex during a Solar Eclipse

Atef Zoughlami[1]

[1]University of Carthage, Tunisia.

Corresponding author: Atef Zoughlami (zoughlamiatef@yahoo.com)

Abstract

Researchers are intensively working to understand the phenomena that remain inadequately explained in connection with solar eclipses, including wind fluctuations, gravity waves, and oscillations in the Foucault pendulum. Despite the numerous theories that have been put up to elucidate these changes, substantial evidence remains necessary to substantiate any of them. Studies indicate that these alterations transpire more frequently at the core of the shadow and are observable throughout all atmospheric strata. Nevertheless, no research has concentrated on thoroughly examining the complete lunar umbra cone, encompassing the influence of the moon's wake phenomena. The lunar umbra cone is a common structure at both ends. This work highlights the parallels between changes in wind and gravity waves during solar eclipses and interplanetary magnetic field (IMF) lines. Building on our analysis, we propose a novel concept that offers a more cohesive and effective explanation of these phenomena during eclipses. This explanation is based on the formation of the magnetic vortex generated by the IMF lines extending from behind the moon to the Earth.

https://doi.org/10.5194/angeo-2024-19
Preprint. Discussion started: 2 December 2024

Annales Geophysicae Discussions
Open Access
EGU

1 Introduction

Solar eclipses arise when the moon intersects the line between the sun and the earth, blocking out sunlight in particular areas of the planet's surface depending on its path. This celestial occurrence gives a singular chance for researchers to observe and examine the consequences of this phenomenon. Several mysterious phenomena appear during this event, for which we still lack a full explanation. Among these phenomena is the Allais (1957) effect, which shows oscillations of the Foucault pendulum during a solar eclipse. This oscillation was regarded as a novel domain distinct from classical gravitational theory. This phenomenon generated global scientific attention, prompting the suggestion of various theories, including the concept that wind and atmospheric pressure alterations may affect the pendulum's oscillations. The hypothesis that the supersonic movement of the moon's shadow could affect the pendulum's oscillations was dismissed. "Eclipse winds" are another poorly understood phenomenon that occurs during a solar eclipse, manifesting as light tornadoes (Aplin and Harrison, 2003; Eaton et al., 1997; Gray and Harrison, 2012) and are distinguished by their unstable wind patterns. During a solar eclipse, ionospheric layers exhibit upward movements, especially in regions of maximum obscuration, accompanied by a significant drift in total electron content (TEC), Furthermore, numerous other variations.

During a solar eclipse, the moon's shadow moves across the Earth's atmosphere, affecting different layers of it (Anderson, 1999). Chimonas & Hins (1970) proposed that the moon's shadow movement, which exceeds the speed of sound has a cooling impact and disrupts the equilibrium of the atmosphere, creating gravity waves. Since then, these waves have received expert attention, and studies have intensified to determine their source. Reports indicate the emergence of gravity waves due to a solar eclipse in various atmospheric areas, derived from disparate observational evidence. Experimental findings demonstrate that gravity waves travel from the stratosphere to the ionosphere, which exhibits low ozone concentrations due to inadequate solar radiation (Fritts and Luo, 1993). Some studies (Altadill et al., 2001; Gerasopoulos et al., 2008; Jakowski et al., 2008; Manju et al., 2012; Šauli et al., 2006) suggest that the ionosphere may generate these waves. Farges et al. (2003) identified two origins for the waves: the thermosphere and the lower atmosphere. These observations are consistent with the work of Šauli et al. (2007), who documented the emission of two waves: one ascending from an altitude of 200 km and the other descending to below 200 km. Gomez (2021) conducted a recent study that demonstrated the vertical travel of these waves through all layers, from the troposphere to the thermosphere, and their potential to reach altitudes exceeding 300 km within the umbra. These waves are known to have several properties, including an increase in amplitude with height (Fritts and Luo, 1993). Jones et al. (2004) stated that the waves synchronize with the moon's shadow, exhibiting increased strength and greater frequency during the phase of maximum obscuration (Lin et al., 2018). This indicates that the eclipse is the origin of these waves and that it synchronizes their movement with the moon's umbra (Nayak and Yiğit, 2018). The evidence suggests that gravity waves are stronger and more intense during the maximum obscuration phase, so it is important to closely examine them to help us understand the mysterious phenomena and changes that occur during a solar eclipse. Initially, we disclose the impact of a solar eclipse on the atmosphere and

https://doi.org/10.5194/angeo-2024-19
Preprint. Discussion started: 2 December 2024

Annales Geophysicae Discussions

the earth's surface, as well as the subsequent events that predominantly occur within the central shadow. Secondly, after examining this literature, we distill the most significant findings and insights regarding the lunar umbra.

2 Experiments and results during a solar eclipse

2.1 Gravity waves and their properties in maximum obscuration

In addition to the property of increasing the wave amplitude with height, we add in this section the most important known features of gravity waves that appear during solar eclipses. According to Šauli et al. (2007), gravity waves manifest vertically, and their propagation direction is oblique, they also discovered that these waves exhibit both upward and downward motion. In his work, Venkat Ratnam et al. (2012) established that the hodograph analysis demonstrated the wave's upward motion and clockwise rotation, along with its downward and counterclockwise rotation. This aligns with Sheng-Yang Gu's (2023) observation that gravity waves show more intensity on the north side of the central eclipse than on the south side. Several studies also address a related topic, observing simultaneous upward and downward energy-pulling processes (Barad and Sripathi, 2023; Chen et al., 2021). Chen et al. (2014) and Manju et al. (2014) uncovered another characteristic of gravity waves, demonstrating its elliptical polarization through their research.

2.2 During the maximum obscuration, the atmosphere changes

Here, we summarize the key details of the variations that occur at different atmospheric layers during a solar eclipse. The data indicate that there has been a discernible drop in ozone levels, particularly during the period of maximum obscuration (Girach et al., 2012; Manchanda et al., 2012; Zerefos et al., 2007). Pradipta et al. (2018) and Chen et al. (2019) indicated a progressive reduction in total electron content (TEC) during the solar eclipse phase. The TEC drop value can reach a maximum of 60% within the umbra (Aa et al., 2020; Coster et al., 2017) this percentage is deemed elevated compared to other locations. Numerous studies have documented clear disturbances in the ionosphere layers during a solar eclipse. For instance, during the 2009 eclipse in China, Gang Chen et al. (2011) observed that gravity waves dragged the ES layer upward. In the same vein, J. Wang et al. (2021) verified that the highest upward lift rate of the ES layer occurs at maximum obscuration in Xiamen, China (24.2°N, 118.07°E, 97.8% obscuration), and it is lower in places where the obscuration ratio is low. The upward pulling process may approach 400 km in the F and E layers, particularly at the core of the eclipse shadow compared to the surrounding areas (Pradipta et al., 2018). According to Martínez et al. (2020), at Temuco station (38.7°S, 72.6°W), the F1 and E ionospheric layers experience the most significant reduction, while the TEC drift and critical frequencies exhibit the highest changes when the obscuration ratio is 100%, in contrast to other stations with lower obscuration ratios. Tian (2022) pointed out the upward movement in the F2 layer during the first stage of entering the lunar shadow and a subsequent decline after the shadow leaves.

During an eclipse, intense gravity waves propagate from the lower atmosphere to the ionosphere, facilitating the occurrence of traveling ionospheric disturbances (TIDS). These TIDS follow the moon's shadow path and appear as curved wavefronts (Jones, 1999; Yan et al., 2021). Sun et al. (2018) examined the emergence of the ionosphere bow

https://doi.org/10.5194/angeo-2024-19
Preprint. Discussion started: 2 December 2024

Annales Geophysicae Discussions
Open Access
EGU

wave as a feature associated with the onset of maximum obscuration. Zhang et al. (2017) state that its structure is elliptical.

2.3 The eclipse cyclone is located within the path of the moon's shadow

The progress made in elucidating the relationship between gravity waves and wind system changes during a solar eclipse, along with their motion characteristics, is summarized in this section. Historically, the solar eclipse of May 28, 1900, that crossed the United States of America marked the beginning of the observation of the eclipse cyclone phenomenon by Clayton (1901), which concluded by noting the appearance of rings rotating in opposite directions from each other around the totality region and differing in radial distance. However, the scientific community at the time did not agree with Clayton's theory (Aplin et al., 2016). Almost a century later, Müller-Wodarg (1998) confirmed that the winds show counterclockwise rotational motion around the low-pressure zone. In the same context, a simulation conducted by Prenosil (2000) of a solar eclipse traversing Europe exhibited similar features to those of an eclipse cyclone. Similarly, Aplin & Harrison's (2003) model closely agrees with the Clayton theory. This model features a chilly core at its center, encircled by a clockwise-rotating ring. It possesses an autonomous internal rotation in a counterclockwise direction, with a diameter of approximately 170 km.

During the maximum obscuration of a solar eclipse in India, researchers detected wind disturbances in two different levels of the atmosphere, accompanied by the elliptical motion of winds. In addition, the investigation revealed the presence of vertical wavelengths in the troposphere that might approach 6 km in wind structure (Ramkumar et al., 2013), as is widely known, gravity waves can create winds (Hines, 1974). In recent studies, the eclipse winds have been better explained based on multiple observations, where they are perpendicular and appear at the first contact by entering the region of totality, persisting alongside the lunar shadow it shows downward winds in the anterior arch and upward winds in the posterior arch at an altitude of 400 km (Cnossen et al., 2019). Piscitelli & Saurral (2021) also observe that when the local area surpasses its maximum obscuration, the speed of these winds increases.

2.4 The elliptical motion of a pendulum occurs at the maximum obscuration

To provide comprehensive insights into the analysis and linking of ideas and observations associated with the solar eclipse, we present in this section the most important experiments of the Foucault pendulum, as some reports must be considered and these individual results cannot be ignored. Researchers have performed independent experiments to observe this impact inside and outside the lunar umbra. During the solar eclipse in Mexico, researchers experimented with a paraconic pendulum, which could rotate about its axis and oscillate in all directions. The experiment occurred in Pato-Branco, located at the lunar umbra, Savrov (1991) noted a pendulum transition from a linear path to an elliptical trajectory. Additionally, the rotation rate increased significantly by three times for the local Foucault effect around the azimuth of the major axis. The observation of elliptical motion is consistent with the findings of Kuusela's (1992) experiment, which was conducted on the same day as Savrov's experiment, specifically in the lunar umbra, during the experiment, the sun's height approached 80°. On November 3, 1994, Savrov repeated the experiment utilizing two pendulums during the maximum obscuration phase of a solar eclipse in Brazil and saw an identical effect. The elliptical motion emerged when the pendulum’s rotation speed increased, surpassing the

https://doi.org/10.5194/angeo-2024-19
Preprint. Discussion started: 2 December 2024

Annales Geophysicae Discussions

local Foucault effect. Despite the clarity of these results, the existence of this effect remained subject to disagreement, as it has been considered that such effects during eclipses may be due to errors in the instruments, measurements, or calculations. However, the observers continued their experiments and monitored the pendulum's movement, as Olenici & Pugach (2012) used a pendulum and a torsion balance during the partial eclipse in their experiment to confirm Allais' observation, their observations revealed convex curves, suggesting this force could rotate the torsion balance. Nonetheless, Olenici et al. (2014) did not settle for that limit, but instead repeated the experiment, reaffirming their results with the presence of the effect.

3 Key observations

This section will emphasize the most intriguing observations noted in the introduction and sections about the impact of solar eclipses on planet Earth. Results show that the largest drift in TEC and critical frequencies occurs after the maximum obscuration, i.e., in the lunar umbra, and this is the region where the highest upward ionospheric drag occurs, as the origin of gravity waves is linked to the lunar umbra, which moves in sync with it. Within this region, gravity waves are characterized by vertical orientation and oblique propagation, and the wave amplitude increases with height. We also observe a high-frequency flow, which gradually decreases in the surrounding regions as we move away from the maximum obscuration. The results also show that the waves rotate clockwise upward and counterclockwise downward. Where the lunar umbra cone contains these waves, Studies have shown that gravity waves within the maximum obscuration have a vertical wavelength of up to 90 km and travel to heights of up to 300 km, allowing them to pass through all layers of the atmosphere. Therefore, the wind structure exhibits vertical structure and elliptical rotation due to the influence of gravity waves. In the same context, the pendulum undergoes an elliptical movement whenever the experiment falls within the maximum obscuration (The lunar umbra).

These observations lead us to consider the possibility that the source of the influence on these waves is outside the atmosphere, specifically in the lunar umbra. The question is whether these waves will ascend further. What types of physical phenomena may manifest in this area? Consequently, we must examine the physical processes occurring within this conical component in general.

4 The modifications in the IMF lines within the lunar umbra

In this section, we will attempt to shed light on the most notable results in the structure of the lunar umbra near the moon, as many studies have demonstrated the formation of a structure directly behind it, known as the lunar wake, upon absorption of the solar wind by the lunar surface, the IMF lines traverse unimpeded to the lunar nightside, thereby forming a complicated structure in that area (Lyon et al., 1967).

The substantial augmentation of the magnetic field, especially within the central lunar wake, is contingent upon the angle of interaction between the solar wind and the IMF lines. In the perpendicular case, the expansion of the IMF is restricted to the nearby moon. In the case of parallel solar winds, there is an increase in the magnetic field, and it extends to long distances downstream (Holmström et al., 2012; Wang et al., 2011; Xie et al., 2013; Zhang et al., 2012). The observed phenomenon results from the electric field surrounding the shadow cone created by the

https://doi.org/10.5194/angeo-2024-19
Preprint. Discussion started: 2 December 2024

Annales Geophysicae Discussions

accelerated motion of electrons behind the moon (Birch and Chapman, 2001, 2002). The electric current creates closed cylinder loops perpendicular to the IMF lines, putting pressure on them as illustrated in Fig 4 of the study by Fatemi et al. (2013). The application of pressure causes the IMF lines to bend, resulting in an axially symmetric configuration centered on the central lunar wake axis (see Fig 1). As a result, it increases the intensity of the magnetic field on the far side of the lunar wake, we also note that there is a rotation of the field attributed to the Mach cone (Michel, 1968; Owen et al., 1996).

Observations suggest that the IMF within the lunar wake (The lunar umbra) exhibits a clockwise rotation at Z>0 and a counterclockwise rotation at Z<0, It is also depicted in Fig 14 of Zhang et al. (2014). On the other hand, the lunar satellite Kaguya observed a reflection of magnetic field rotation between the Northern and Southern Hemispheres at a 90° angle in the lunar wake, i.e., in the lunar umbra. Simultaneously, solar winds were found to align parallel to the magnetic field, and the polarization exhibited an extremely elliptical nature (Nakagawa et al., 2021).

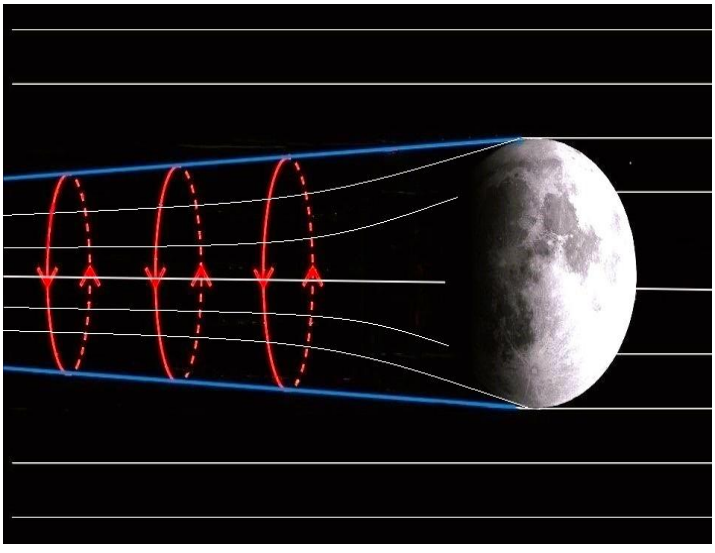

Figure 1: The white lines represent IMF, and as they pass the moon, the electrical current indicated by the red rings forces these lines to bend at the edges of the Umbra lunar cone, as illustrated by the two blue lines.

5 Similarities

This section will compare the results and observations gathered regarding gravity waves and the IMF. On the lunar nightside, the IMF lines are bent inward, which leads to a significant increase in the expansion of the magnetic field downstream. First, this bending is consistent with gravity waves' oblique propagation and vertical direction during a solar eclipse. Second, the stretched IMF and the high-frequency gravity waves share in the umbra cone. Another comparison reveals that the IMF lines behind the moon which represents the lunar umbra cone, rotate in two directions: clockwise and counterclockwise, signifying a push and pull force, that aligns with the upward and

https://doi.org/10.5194/angeo-2024-19
Preprint. Discussion started: 2 December 2024

Annales Geophysicae Discussions
Open Access
EGU

downward motion of gravity waves and the wind movement during the maximum obscuration phase. On the other hand, the satellite Kaguya results indicate the presence of an elliptical motion behind the moon at an angle of 90°, which is consistent with the elliptical polarization of gravity waves, which in turn stimulates the elliptical motion of the winds. In addition, this result is consistent with the elliptical motion of the Foucault pendulum when the obscuration ratio is 100% (the lunar umbra). The temporal dependence in comparing the duration of disturbances and oscillations during the eclipse with the vibration period in the IMF structure behind the moon is also significant. This comparison relies on data obtained by the ARTEMIS mission, which indicated that the duration ranged from 5 to 60 minutes on the edge of the lunar wake (Poppe et al., 2014). Researchers typically estimate this period to be between 40 and 60 minutes after the eclipse maximum (Altadill et al., 2001; Chen et al., 2015; Farges et al., 2003; Wang et al., 2021), highlighting the importance of this time in analyzing atmospheric fluctuations during eclipses.

6 Discussion and conclusions

The IMF lines are similar to magnetohydrodynamics (MHD) in that they interact with the solar wind and other matter in space. As a result of this interaction, the magnetic field lines can become curved, becoming parallel, creating what is known as magnetic vortices (Durand-Manterola and Flandes, 2022). It is known in scientific circles that the pressure of electric current on vertical magnetic lines, when they are in the form of closed loops leads to the bending of these lines, which become parallel around a fixed axis and end in the form of a vortex. Thus, this description is consistent with the pressure exerted by the electric current in space on the IMF lines, causing them to bend inward (refer to sectional figure 2). This increases the expansion of the magnetic field in the central lunar wake axis, which means a magnetic vortex. Observing the Kaguya satellite, which showed an elliptical rotation at a 90° angle within the center of the wake, confirms the formation of a magnetic vortex behind the moon.

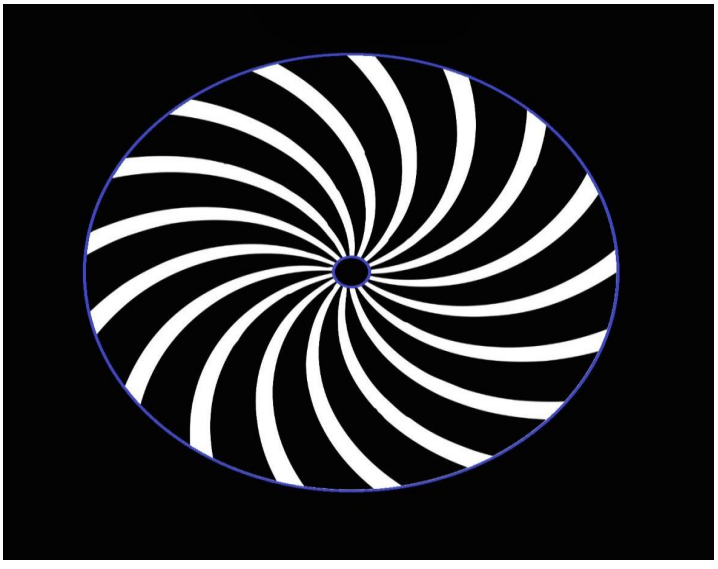

https://doi.org/10.5194/angeo-2024-19
Preprint. Discussion started: 2 December 2024

Annales Geophysicae Discussions
Open Access
EGU

Figure 2: Depicts a cross-section of the lunar umbra cone, with the white color indicating the symmetrical and curved IMF lines, the large blue circle representing the cone's boundaries, and the small circle representing the shadow's center (The maximum obscuration).

It is worth noting that the IMF lines at the edges of the lunar umbra cone rotate in two directions: clockwise and counterclockwise, indicating a push and pull force. This interaction is also an indicator of the presence of a magnetic vortex. From this perspective, we can examine the lowest section of this cone as a shared component of the lunar umbra. By identifying common characteristics, we intend to demonstrate that vortex structure may extend to the atmosphere and the Earth's surface. Models of vortex formation can elucidate this pattern, especially when considering the effects of magnetic fields.

Our literature has noted the elliptical motion of gravity waves and winds in the atmosphere during eclipses. Additionally, the pendulum experiences elliptical motion as its rotation rate increases. This rotation property is regarded as one of the fundamentals of the vortex, providing an essential explanation for the core of any vortex, which represents the umbra region. A dominant feature of vortices is their coordinated upward and downward motion, indicating a clockwise direction during ascent and a counterclockwise direction during descent. This property is consistent during eclipses with the motion of IMF lines, gravity waves, and winds even at altitudes of up to 400 km around the region of totality. Furthermore, in vortices or tornadoes, an intersection exists between phase motion and energy transfer, as energy accumulates and delineates a certain trajectory (such as the descent of cold air). At the same time, other structural components revolve circularly around the center. This leads us to the research indicating that cold air descends on the umbra area during a solar eclipse, replacing warm air (Elmhamdi et al., 2024). This serves as additional evidence of the presence of a vortex structure in the atmosphere.

Given our reliance on models of cyclones and magnetic vortices for comparison, we can highlight the effect of the vortex and its magnetic field on charged particles. This field forces the particles to move in helical paths within this conical structure at an inclined angle, forming a structure similar to the motion of these particles within it. Additionally, this field can elevate plasma to higher layers, increasing its flow toward upper regions. Some studies have indicated the occurrence of this phenomenon in the atmosphere, particularly around the shadow center. For instance, Wang et al. (2019) noted that winds near the shadow center contribute to lifting plasma upward, altering its density. Moreover, Tian et al. (2022) demonstrated that the F2 layer exhibited a tilted structure, with plasma rising in the west while decreasing in the east. The results also showed that plasma ascended during the initial contact of the obscuration phase. In this context, a study by Manju et al. (2014) revealed that horizontal winds exhibit an inclined elliptical shape, based on hodograph analysis of the ionospheric E layer. These findings are supported by studies by Jie Wang et al. (2023) and Chi-Yen Lin et al. (2021) The former reported ascending and descending echo structures with inclined geometry during the solar eclipse on June 21, 2020, while the latter suggested that the moon's shadow could cause horizontal tilting in the ionosphere. These studies reflect ascending and descending fields at inclined angles, which aligns with the concept of a magnetic vortex structure. Thus, we believe that the changes in gravity waves, winds, and the Allais effect during a solar eclipse are mostly attributable to the IMF lines inside the lunar umbra cone. We consider IMF lines can affect charged particles by moving them toward the upper

https://doi.org/10.5194/angeo-2024-19
Preprint. Discussion started: 2 December 2024

Annales Geophysicae Discussions
Open Access
EGU

232 layers, creating atmospheric pressure, and thus causing variations in wind patterns and gravity waves. Since the IMF
233 lines are vortex-shaped, they force the wind to direct its movement as a cyclone.

234 The lower temperature and the velocity of the moon's shadow are frequently posited as the primary variables
235 contributing to the oscillations observed during a solar eclipse. A series of accurate measurements in China utilizing
236 the Lacoste-Romberg gravimeter during the solar eclipse on March 9, 1997, indicated a reduction in the gravity
237 value of approximately 0.7 millionths of a percent of the standard gravity value (Yang and Wang, 2002). This
238 reduction was attributed to the supersonic transit of the moon's shadow, temperature, and barometric pressure
239 fluctuations. Despite barometric pressure, the influence of the moving shadow in the atmosphere remains a hundred
240 thousand times insufficient to account for the retrograde motion of a pendulum (Bagdoo, 2023).

241 From the perspective of theoretical analysis, It is believed that the start of darkness induces a decrease in
242 temperature, resulting in the cooling of the ozone layer and subsequently the emergence of gravity waves. We wish
243 to cite a comparable instance, the Terminator, which traverses at a velocity exceeding the speed of sound before
244 dusk. The absence of light lowers the environment's temperature and facilitates the generation of standard gravity
245 waves. Nevertheless, these waves are often less intense and less pronounced, exhibiting a maximum vertical
246 wavelength of 30 km (Preusse et al., 2002). They can ascend to the mesosphere under optimal atmospheric
247 conditions, although the cooling duration exceeds the maximum obscuration phase of a solar eclipse. Conversely,
248 gravity waves are more intense during a solar eclipse, propagating vertically and horizontally and attaining greater

https://doi.org/10.5194/angeo-2024-19
Preprint. Discussion started: 2 December 2024

Annales Geophysicae Discussions
Open Access
EGU

heights. As stated in Section 2.3, these waves also contribute to the associated consequences of winds. The manifestation of elliptical motion in the umbra should also be noted.

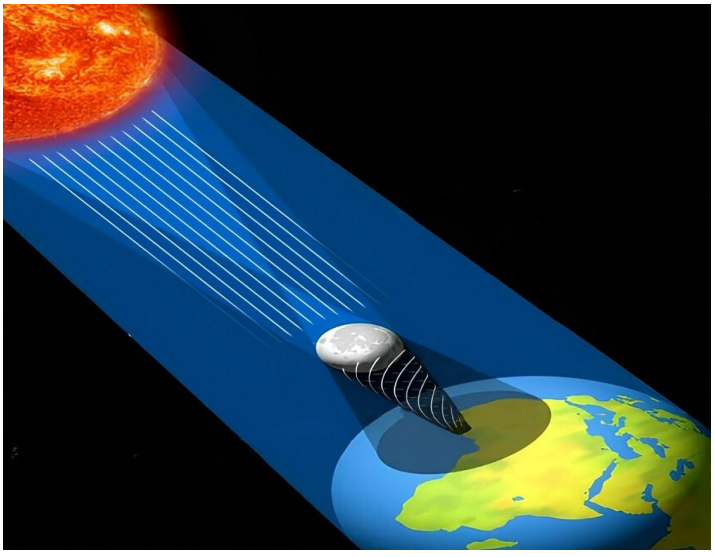

Figure 3: The white lines represent the IMF. After crossing the moon, they bend inward to form a magnetic vortex structure at the edges of the lunar umbra cone, which extends to the Earth.

Our comparison reveals a distinct resemblance and motion consistency between the IMF lines, the gravity, and the changes in the winds inside the lunar umbra cone. Figure 3 shows our perspective based on the analysis of observations, where we suggest that during the solar eclipse, there is a magnetic vortex stretching from the region behind the moon to the Earth's surface. Conical vortices are common in nature. Examples include solar magnetic tornadoes and plasma vortices flowing in strong magnetic fields, such as those found in black holes or electrical discharges in nuclear fusion experiments.

According to our proposal, this conical structure moves in tandem with the lunar umbra cone, with the leading edge functioning as an arched barrier of rising IMF lines, thereby influencing the atmospheric layers, the idea of a magnetic vortex fits with the Clayton cyclone theory that was seen during a solar eclipse. This conclusion also fits with the concept proposed by Olenici et al. (2014), who say solar influences cause a vortex-like effect during the eclipse phase. However, they did not explain the reasons behind this phenomenon and its formation.

Through this combination of observations in outer space, the atmosphere, and on the Earth's surface, this study presents evidence that the IMF lines link to the Earth during a solar eclipse, forming a vortex at the edges of the lunar umbra cone. This paper is the first work to indicate the existence of a magnetic vortex during a solar eclipse, so we consider it suitable for future experimental applications to verify this concept. Therefore, we suggest examining the elliptical motion at two or three altitudes within the lunar umbra cone. The first method involves

https://doi.org/10.5194/angeo-2024-19
Preprint. Discussion started: 2 December 2024

Annales Geophysicae Discussions
Open Access
EGU

conducting a pendulum experiment on the earth's surface, the second involves using balloons or rockets inside the atmosphere, and the third method consists of having a satellite outside the atmosphere, and making sure that the three experiments happen at the same time and on the same vertical path. We recommend selecting the height of the Sun during the eclipse closer to 90°. We should also consider other factors that may affect the structure of the vortex, such as the earth's position in the year, the speed of the solar wind, the time of day, and geography. Therefore, the recurrence of the elliptical motion at these three points can prove the validity of this theory. This theory is anticipated to establish a new avenue for researchers to explore the interaction of IMF lines within the atmosphere and utilize the magnetic vortex structure to elucidate numerous poorly known phenomena that transpire during solar eclipses.

Data Availability Statement

This study does not require data sharing because it relies solely on theoretical analysis and does not create or analyze any new data.

Competing interests

The contact author has declared that none of the authors has any competing interests.

References

Aa, E., Zhang, S. R., Erickson, P. J., Goncharenko, L. P., Coster, A. J., Jonah, O. F., Lei, J., Huang, F., Dang, T., and Liu, L.: Coordinated Ground-Based and Space-Borne Observations of Ionospheric Response to the Annular Solar Eclipse on 26 December 2019, J. Geophys. Res. Sp. Phys., 125, 1–17, https://doi.org/10.1029/2020JA028296, 2020.

Allais, M.: Mouvement du pendule paraconique et éclipse totale de Soleil du 30 juin 1954, in: French Academy of Sciences, vol. 245, 2001-2003., 1957.

Altadill, D., Solé, J. G., and Apostolov, E. M.: Vertical structure of a gravity wave like oscillation in the ionosphere generated by the solar eclipse of August 11, 1999, J. Geophys. Res. Sp. Phys., 106, 21419–21428, https://doi.org/10.1029/2001ja900069, 2001.

Anderson, J.: Meteorological changes during a solar eclipse, Weather, 54, 207–215, https://doi.org/10.1002/j.1477-8696.1999.tb06465.x, 1999.

Aplin, K. L. and Harrison, R. G.: Meteorological effects of the eclipse of 11 August 1999 in cloudy and clear conditions, Proc. R. Soc. A Math. Phys. Eng. Sci., 459, 353–371, https://doi.org/10.1098/rspa.2002.1042, 2003.

Aplin, K. L., Scott, C. J., and Gray, S. L.: Atmospheric changes from solar eclipses, Philos. Trans. R. Soc. A Math. Phys. Eng. Sci., 374, https://doi.org/10.1098/rsta.2015.0217, 2016.

Bagdoo, R.: Is the Growth of the Astronomical Unit Caused by the Allais Eclipse Effect?, J. Mod. Phys., 14, 127–146, https://doi.org/10.4236/jmp.2023.142009, 2023.

Barad, R. K. and Sripathi, S.: Investigation of gravity wave characteristics in the equatorial ionosphere during the passage of the 15 January 2010 solar eclipse over Tirunelveli, Adv. Sp. Res., 71, 160–175, https://doi.org/10.1016/j.asr.2022.08.059, 2023.

Birch, P. C. and Chapman, S. C.: Particle-in-cell simulations of the lunar wake with high phase space resolution,

https://doi.org/10.5194/angeo-2024-19
Preprint. Discussion started: 2 December 2024

306 Geophys. Res. Lett., 28, 219–222, https://doi.org/10.1029/2000GL011958, 2001.
307 Birch, P. C. and Chapman, S. C.: Two dimensional particle-in-cell simulations of the lunar wake, Phys. Plasmas, 9,
308 1785, https://doi.org/10.1063/1.1467655, 2002.
309 Chen, C. H., Lin, C. H. C., and Matsuo, T.: Ionospheric responses to the 21 August 2017 solar eclipse by using data
310 assimilation approach, Prog. Earth Planet. Sci., 6, 1–9, https://doi.org/10.1186/s40645-019-0263-4, 2019.
311 Chen, G., Zhao, Z., Zhang, Y., Yang, G., Zhou, C., Huang, S., Li, T., Li, N., and Sun, H.: Gravity waves and spread
312 Es observed during the solar eclipse of 22 July 2009, J. Geophys. Res. Sp. Phys., 116, 1–7,
313 https://doi.org/10.1029/2011JA016720, 2011.
314 Chen, G., Wu, C., Zhao, Z., Zhong, D., Qi, H., and Jin, H.: Daytime e region field-aligned irregularities observed
315 during a solar eclipse, J. Geophys. Res. Sp. Phys., 119, 10,633-10,640, https://doi.org/10.1002/2014JA020666,
316 2014.
317 Chen, G., Wu, C., Huang, X., Zhao, Z., Zhong, D., Qi, H., Huang, L., Qiao, L., and Wang, J.: Plasma flux and
318 gravity waves in the midlatitude ionosphere during the solar eclipse of 20 May 2012, J. Geophys. Res. Sp. Phys.,
319 120, 3009–3020, https://doi.org/10.1002/2014JA020849, 2015.
320 Chen, G., Wang, J., Reinisch, B. W., Li, Y., and Gong, W.: Disturbances in Sporadic-E During the Great Solar
321 Eclipse of August 21, 2017, J. Geophys. Res. Sp. Phys., 126, https://doi.org/10.1029/2020JA028986, 2021.
322 Chimonas, G. and Hines, C. O.: Atmospheric gravity waves induced by a solar eclipse, J. Geophys. Res., 75, 875–
323 875, https://doi.org/10.1029/ja075i004p00875, 1970.
324 Clayton, H. H.: The eclipse cyclone, the diurnal cyclones, and the cyclones and anticyclones of temperate latitudes,
325 Q. J. R. Meteorol. Soc., 27, 269–292, https://doi.org/10.1002/qj.49702712004, 1901.
326 Cnossen, I., Ridley, A. J., Goncharenko, L. P., and Harding, B. J.: The Response of the Ionosphere-Thermosphere
327 System to the 21 August 2017 Solar Eclipse, J. Geophys. Res. Sp. Phys., 124, 7341–7355,
328 https://doi.org/10.1029/2018JA026402, 2019.
329 Coster, A. J., Goncharenko, L., Zhang, S. R., Erickson, P. J., Rideout, W., and Vierinen, J.: GNSS Observations of
330 Ionospheric Variations During the 21 August 2017 Solar Eclipse, Geophys. Res. Lett., 44, 12,041-12,048,
331 https://doi.org/10.1002/2017GL075774, 2017.
332 Durand-Manterola, H. J. and Flandes, A.: Plasma vortices driven by magnetic torsion generated by electric currents
333 in non-magnetic planetary wakes, Adv. Sp. Res., 69, 3902–3908, https://doi.org/10.1016/j.asr.2022.03.002, 2022.
334 Eaton, F. D., Hines, J. R., Hatch, W. H., Cionco, R. M., Byers, J., Garvey, D., and Miller, D. R.: Solar eclipse effects
335 observed in the planetary boundary layer over a desert, Boundary-Layer Meteorol., 83, 331–346,
336 https://doi.org/10.1023/A:1000219210055, 1997.
337 Elmhamdi, A., Roman, M. T., Peñaloza-Murillo, M. A., Pasachoff, J. M., Liu, Y., Al-Mostafa, Z. A., Maghrabi, A.
338 H., Oloketuyi, J., and Al-Trabulsy, H. A.: Impact of the Eclipsed Sun on Terrestrial Atmospheric Parameters in
339 Desert Locations: A Comprehensive Overview and Two Events Case Study in Saudi Arabia †, Atmosphere (Basel).,
340 15, https://doi.org/10.3390/atmos15010062, 2024.
341 Farges, T., Le Pichon, A., Blanc, E., Perez, S., and Alcoverro, B.: Response of the lower atmosphere and the
342 ionosphere to the eclipse of August 11, 1999, J. Atmos. Solar-Terrestrial Phys., 65, 717–726,

https://doi.org/10.5194/angeo-2024-19
Preprint. Discussion started: 2 December 2024

Annales Geophysicae Discussions
Open Access
EGU

https://doi.org/10.1016/S1364-6826(03)00078-6, 2003.

Fatemi, S., Holmström, M., Futaana, Y., Barabash, S., and Lue, C.: The lunar wake current systems, Geophys. Res. Lett., 40, 17–21, https://doi.org/10.1029/2012GL054635, 2013.

Fritts, D. C. and Luo, Z.: Gravity wave forcing in the middle atmosphere due to reduced ozone heating during a solar eclipse, J. Geophys. Res., 98, 3011–3021, https://doi.org/10.1029/92JD02391, 1993.

Gerasopoulos, E., Zerefos, C. S., Tsagouri, I., Founda, D., Amiridis, V., Bais, A. F., Belehaki, A., Christou, N., Economou, G., Kanakidou, M., Karamanos, A., Petrakis, M., and Zanis, P.: The total solar eclipse of March 2006: Overview, Atmos. Chem. Phys., 8, 5205–5220, https://doi.org/10.5194/acp-8-5205-2008, 2008.

Girach, I. A., Nair, P. R., David, L. M., Hegde, P., Mishra, M. K., Kumar, G. M., Das, S. M., Ojha, N., and Naja, M.: The changes in near-surface ozone and precursors at two nearby tropical sites during annular solar eclipse of 15 January 2010, J. Geophys. Res. Atmos., 117, 1–14, https://doi.org/10.1029/2011JD016521, 2012.

Gómez, D. D.: Ionospheric Response to the December 14, 2020 Total Solar Eclipse in South America, J. Geophys. Res. Sp. Phys., 126, 1–14, https://doi.org/10.1029/2021JA029537, 2021.

Gray, S. L. and Harrison, R. G.: Diagnosing eclipse-induced wind changes, Proc. R. Soc. A Math. Phys. Eng. Sci., 468, 1839–1850, https://doi.org/10.1098/rspa.2012.0007, 2012.

Gu, S. Y., Yang, Z., Qin, Y., Teng, C. K. M., Dou, X., Lei, J., Huang, F., Dang, T., and Sun, W.: Ionospheric TEC Variation and Gravity Waves Signatures During the Solar Eclipse on 21 June 2020 Over Southern China, J. Geophys. Res. Sp. Phys., 128, 1–15, https://doi.org/10.1029/2022JA030758, 2023.

Hines, C. O.: The upper atmosphere in motion, in The Upper Atmosphere in Motion, Geophys. Monogr. Ser., in: AGU, vol. 18, Washington, D.C, 31–39, 1974.

Holmström, M., Fatemi, S., Futaana, Y., and Nilsson, H.: The interaction between the Moon and the solar wind, Earth, Planets Sp., 64, 237–245, https://doi.org/10.5047/eps.2011.06.040, 2012.

Jakowski, N., Stankov, S. M., Wilken, V., Borries, C., Altadill, D., Chum, J., Buresova, D., Boska, J., Sauli, P., Hruska, F., and Cander, L. R.: Ionospheric behavior over Europe during the solar eclipse of 3 October 2005, J. Atmos. Solar-Terrestrial Phys., 70, 836–853, https://doi.org/10.1016/j.jastp.2007.02.016, 2008.

Jones, B. W.: A search for atmospheric pressure waves from the total solar eclipse of 9 March 1997, J. Atmos. Solar-Terrestrial Phys., 61, 1017–1024, https://doi.org/10.1016/S1364-6826(99)00073-5, 1999.

Jones, T. B., Wright, D. M., Milner, J., Yeoman, T. K., Reid, T., Chapman, P. J., and Senior, A.: The detection of atmospheric waves produced by the total solar eclipse of 11 August 1999, J. Atmos. Solar-Terrestrial Phys., 66, 363–374, https://doi.org/10.1016/j.jastp.2004.01.029, 2004.

Kuusela, T.: New measurements with a torsion pendulum during the solar eclipse, Gen. Relativ. Gravit., 24, 543–550, https://doi.org/10.1007/BF00760136, 1992.

Lin, C. Y., Deng, Y., and Ridley, A.: Atmospheric Gravity Waves in the Ionosphere and Thermosphere During the 2017 Solar Eclipse, Geophys. Res. Lett., 45, 5246–5252, https://doi.org/10.1029/2018GL077388, 2018.

Lin, C. Y., Liu, J. Y., Sun, Y. Y., Lin, C. C. H., Chang, L. C., Chen, C. Y., and Chen, C. H.: Ionospheric tilting of 21 August 2017 total solar eclipse sounded by GNSS ground-based receivers and radio occultation, Terr. Atmos. Ocean. Sci., 32, 531–539, https://doi.org/10.3319/TAO.2021.08.17.01, 2021.

https://doi.org/10.5194/angeo-2024-19
Preprint. Discussion started: 2 December 2024

380 Lyon, E. F., Bridge, and Binsack: Explorer 35 plasma measurements in the vicinity of the Moon, J. Geophys. Res.,
381 72, 6113–6117, https://doi.org/10.1029/jz072i023p06113, 1967.
382 Manchanda, R. K., Sinha, P. R., Sreenivasan, S., Trivedi, D. B., Kapardhi, B. V. N., Suneel Kumar, B., Kumar, P.
383 R., Satyaprakash, U., and Rao, V. N.: In-situ measurements of vertical structure of ozone during the solar eclipse of
384 15 January 2010, J. Atmos. Solar-Terrestrial Phys., 84–85, 88–100, https://doi.org/10.1016/j.jastp.2012.05.011,
385 2012.
386 Manju, G., Sridharan, R., Ravindran, S., Madhav Haridas, M. K., Pant, T. K., Sreelatha, P., and Mohan Kumar, S.
387 V.: Rocket borne in-situ Electron density and Neutral Wind measurements in the equatorial ionosphere-Results from
388 the January 2010 annular solar eclipse campaign from India, J. Atmos. Solar-Terrestrial Phys., 86, 56–64,
389 https://doi.org/10.1016/j.jastp.2012.06.009, 2012.
390 Manju, G., Haridas, M. K. M., G. Ramkumar, T. K. P., Sridharan, R., and Sreelatha, P.: Gravity wave signatures in
391 the dip equatorial ionosphere-thermosphere system during the annular solar eclipse of 15 January 2010, J. Geophys.
392 Res. Sp. Phys., 119, 4929–4937, https://doi.org/10.1002/2014JA019865, 2014.
393 Martínez-Ledesma, M., Bravo, M., Urra, B., Souza, J., and Foppiano, A.: Prediction of the Ionospheric Response to
394 the 14 December 2020 Total Solar Eclipse Using SUPIM-INPE, J. Geophys. Res. Sp. Phys., 125, 1–11,
395 https://doi.org/10.1029/2020JA028625, 2020.
396 Michel, F. C.: Magnetic field structure behind the Moon, J. Geophys. Res., 73, 1533–1542,
397 https://doi.org/10.1029/ja073i005p01533, 1968.
398 Müller-Wodarg, I. C. F., Aylward, A. D., and Lockwood, M.: Effects of a mid-latitude solar eclipse on the
399 thermosphere and ionosphere - a modelling study, Geophys. Res. Lett., 25, 3787–3790,
400 https://doi.org/10.1029/1998GL900045, 1998.
401 Nakagawa, T., Takahashi, F., Saito, Y., and Shimizu, H.: Polarization Reversal of Low-Frequency Magnetic
402 Variation in the Lunar Wake, J. Geophys. Res. Sp. Phys., 126, https://doi.org/10.1029/2021JA029299, 2021.
403 Nayak, C. and Yiğit, E.: GPS-TEC Observation of Gravity Waves Generated in the Ionosphere During 21 August
404 2017 Total Solar Eclipse, J. Geophys. Res. Sp. Phys., 123, 725–738, https://doi.org/10.1002/2017JA024845, 2018.
405 Olenici, D. and Pugach, A. F.: Precise Underground Observations of the Partial Solar Eclipse of 1 June 2011 Using
406 a Foucault Pendulum and a Very Light Torsion Balance, Int. J. Astron. Astrophys., 02, 204–209,
407 https://doi.org/10.4236/ijaa.2012.24026, 2012.
408 Olenici, D., Pugach, A. F., Cosovanu, I., Lesanu, C., Deloly, J.-B., Vorobyov, D., Delets, A., and Olenici-
409 Craciunescu, S.-B.: Syzygy Effects Studies Performed Simultaneously with Foucault Pendulums and Torsinds
410 during the Solar Eclipses of 13 November 2012 and 10 May 2013, Int. J. Astron. Astrophys., 04, 39–53,
411 https://doi.org/10.4236/ijaa.2014.41006, 2014.
412 Owen, C. J., Lepping, R. P., Ogilvie, K. W., Slavin, J. A., Farrell, W. M., and Byrnes, J. B.: The lunar wake at 6.8
413 RL: WIND magnetic field observations, Geophys. Res. Lett., 23, 1263–1266, https://doi.org/10.1029/96GL01354,
414 1996.
415 Piscitelli, F. M. and Saurral, R. I.: The total solar eclipse of December 14, 2020 in southern South America and its
416 effects on atmospheric variables, Q. J. R. Meteorol. Soc., 147, 2547–2561, https://doi.org/10.1002/qj.4040, 2021.

https://doi.org/10.5194/angeo-2024-19
Preprint. Discussion started: 2 December 2024

417 Poppe, A. R., Fatemi, S., Halekas, J. S., Holmström, M., and Delory, G. T.: ARTEMIS observations of extreme
418 diamagnetic fields in the lunar wake, Geophys. Res. Lett., 41, 3766–3773, https://doi.org/10.1002/2014GL060280,
419 2014.
420 Pradipta, R., Yizengaw, E., and Doherty, P.: Ionospheric Density Irregularities, Turbulence, and Wave Disturbances
421 During the Total Solar Eclipse Over North America on 21 August 2017, Geophys. Res. Lett., 45, 7909–7917,
422 https://doi.org/10.1029/2018GL079383, 2018.
423 Prenosil, T.: The influence of the 11 August 1999 total solar eclipse on the weather over central Europe, Meteorol.
424 Zeitschrift, 9, 351–359, https://doi.org/10.1127/metz/9/2000/351, 2000.
425 Preusse, P., Dörnbrack, A., Eckermann, S. D., Riese, M., Schaeler, B., Bacmeister, J. T., Broutman, D., and
426 Grossmann, K. U.: Space-based measurements of stratospheric mountain waves by CRISTA 1. Sensitivity, analysis
427 method, and a case study, J. Geophys. Res. Atmos., 107, https://doi.org/10.1029/2001JD000699, 2002.
428 Ramkumar, G., Subrahmanyam, K. V., Kumar, K. K., Shankar Das, S., Swain, D., Sunilkumar, S. V., Namboodiri,
429 K. V. S., Uma, K. N., Babu, V. S., John, S. R., and Babu, A.: First observational study during a solar eclipse event
430 on variations in the horizontal winds simultaneously in the troposphere-stratospheremesosphere-lower-thermosphere
431 region over the equatorial station Thumba (8.5°N, 77°E), Earth, Planets Sp., 65, 781–790,
432 https://doi.org/10.5047/eps.2012.12.007, 2013.
433 Šauli, P., Abry, P., Boška, J., and Duchayne, L.: Wavelet characterisation of ionospheric acoustic and gravity waves
434 occurring during the solar eclipse of August 11, 1999, J. Atmos. Solar-Terrestrial Phys., 68, 586–598,
435 https://doi.org/10.1016/j.jastp.2005.03.024, 2006.
436 Šauli, P., Roux, S. G., Abry, P., and Boška, J.: Acoustic-gravity waves during solar eclipses: Detection and
437 characterization using wavelet transforms, J. Atmos. Solar-Terrestrial Phys., 69, 2465–2484,
438 https://doi.org/10.1016/j.jastp.2007.06.012, 2007.
439 Savrov, L. A.: Improved determination of variation of rate of rotation of oscillation plane of a paraconic pendulum
440 during the solar eclipse in Mexico on July 11, 1991, Meas. Tech., 52, 339–343, https://doi.org/10.1007/s11018-009-
441 9291-6, 1991.
442 Sun, Y. Y., Liu, J. Y., Lin, C. C. H., Lin, C. Y., Shen, M. H., Chen, C. H., Chen, C. H., and Chou, M. Y.:
443 Ionospheric Bow Wave Induced by the Moon Shadow Ship Over the Continent of United States on 21 August 2017,
444 Geophys. Res. Lett., 45, 538–544, https://doi.org/10.1002/2017GL075926, 2018.
445 Tian, Z., Sui, Y., Zhu, S., and Sun, Y. Y.: Enhancement of Electron Density in the Ionospheric F2 Layer Near the
446 First Contact of the Total Solar Eclipse on 21 August 2017, Earth Sp. Sci., 9,
447 https://doi.org/10.1029/2021EA002016, 2022.
448 Venkat Ratnam, M., Eswaraiah, S., Leena, P. P., Patra, A. K., Krishna Murthy, B. V., and Vijaya Bhaskara Rao, S.:
449 Effect of the annular solar eclipse of 15 January 2010 on the low latitude mesosphere, J. Atmos. Solar-Terrestrial
450 Phys., 80, 340–346, https://doi.org/10.1016/j.jastp.2012.02.022, 2012.
451 Wang, J., Zuo, X., Sun, Y. Y., Yu, T., Wang, Y., Qiu, L., Mao, T., Yan, X. X., Yang, N., Qi, Y., Lei, J., Sun, L., and
452 Zhao, B.: Multilayered Sporadic-E Response to the Annular Solar Eclipse on June 21, 2020, Sp. Weather, 19, 1–9,
453 https://doi.org/10.1029/2020SW002643, 2021.

https://doi.org/10.5194/angeo-2024-19
Preprint. Discussion started: 2 December 2024

Annales Geophysicae Discussions
Open Access
EGU

454 Wang, J., Chen, G., Zhang, S., Zhang, W., He, Z., Huang, K., and Huang, C.: Mid-Latitude Mesospheric Responses
455 of the Solar Eclipse on 21 June 2020 Observed by the Wuhan MST Radar, J. Geophys. Res. Sp. Phys., 128,
456 https://doi.org/10.1029/2022JA030892, 2023.
457 Wang, W., Dang, T., Lei, J., Zhang, S., Zhang, B., and Burns, A.: Physical Processes Driving the Response of the F
458 2 Region Ionosphere to the 21 August 2017 Solar Eclipse at Millstone Hill, J. Geophys. Res. Sp. Phys., 124, 2978–
459 2991, https://doi.org/10.1029/2018JA025479, 2019.
460 Wang, Y. C., Müller, J., Ip, W. H., and Motschmann, U.: A 3D hybrid simulation study of the electromagnetic field
461 distributions in the lunar wake, Icarus, 216, 415–425, https://doi.org/10.1016/j.icarus.2011.09.021, 2011.
462 Xie, L. H., Li, L., Zhang, Y. T., and de Zeeuw, D. L.: Three-dimensional MHD simulation of the lunar wake, Sci.
463 China Earth Sci., 56, 330–338, https://doi.org/10.1007/s11430-012-4383-6, 2013.
464 Yan, M., Dang, T., Lei, J., Wang, W., Zhang, S. R., and Le, H.: From Bow Waves to Traveling Atmospheric
465 Disturbances: Thermospheric Perturbations Along Solar Eclipse Trajectory, J. Geophys. Res. Sp. Phys., 126, 1–12,
466 https://doi.org/10.1029/2020JA028523, 2021.
467 Yang, X. S. and Wang, Q. S.: Gravity anomaly during the Mohe total solar eclipse and new constraint on
468 gravitational shielding parameter, Astrophys. Space Sci., 282, 245–253, https://doi.org/10.1023/A:1021119023985,
469 2002.
470 Zerefos, C. S., Gerasopoulos, E., Tsagouri, I., Psiloglou, B. E., Belehaki, A., Herekakis, T., Bais, A., Kazadzis, S.,
471 Eleftheratos, C., Kalivitis, N., and Mihalopoulos, N.: Evidence of gravity waves into the atmosphere during the
472 March 2006 total solar eclipse, Atmos. Chem. Phys., 7, 4943–4951, https://doi.org/10.5194/acp-7-4943-2007, 2007.
473 Zhang, H., Khurana, K. K., Zong, Q. G., Kivelson, M. G., Hsu, T. S., Wan, W. X., Pu, Z. Y., Angelopoulos, V.,
474 Cao, X., Wang, Y. F., Shi, Q. Q., Liu, W. L., Tian, A. M., and Tang, C. L.: Outward expansion of the lunar wake:
475 ARTEMIS observations, Geophys. Res. Lett., 39, 1–7, https://doi.org/10.1029/2012GL052839, 2012.
476 Zhang, H., Khurana, K. K., Kivelson, M. G., Angelopoulos, V., Wan, W. X., Liu, L. B., Zong, Q. G., Pu, Z. Y., Shi,
477 Q. Q., and Liu, W. L.: Three-dimensional lunar wake reconstructed from ARTEMIS data, J. Geophys. Res. Sp.
478 Phys., 119, 5220–5243, https://doi.org/10.1002/2014JA020111, 2014.
479 Zhang, S. R., Erickson, P. J., Goncharenko, L. P., Coster, A. J., Rideout, W., and Vierinen, J.: Ionospheric Bow
480 Waves and Perturbations Induced by the 21 August 2017 Solar Eclipse, Geophys. Res. Lett., 44, 12,067-12,073,
481 https://doi.org/10.1002/2017GL076054, 2017.
482